Contents lists available at ScienceDirect

Physics Letters B

www.elsevier.com/locate/physletb

PHYSICS LETTERS B

Statefinder diagnosis for Ricci dark energy

Chao-Jun Feng [a,b,*]

[a] _Institute of Theoretical Physics, CAS, Beijing 100080, PR China_
[b] _Interdisciplinary Center for Theoretical Study, USTC, Hefei, Anhui 230026, PR China_

A R T I C L E   I N F O

A B S T R A C T

Statefinder diagnostic is a useful method which can differ one dark energy model from each others. In this Letter, we apply this method to a holographic dark energy model from Ricci scalar curvature, called the Ricci dark energy model (RDE). We plot the evolutionary trajectories of this model in the statefinder parameter-planes, and it is found that the parameter of this model plays a significant role from the statefinder viewpoint. In a very special case, the statefinder diagnostic fails to discriminate LCDM and RDE models, thus we apply a new diagnostic called the _Om_ diagnostic proposed recently to this model in this case in Appendix A and it works well.

1. Introduction

The accelerating cosmic expansion first inferred from the observations of distant type Ia supernovae [1] has strongly confirmed by some other independent observations, such as the cosmic microwave background radiation (CMBR) [2] and Sloan Digital Sky Survey (SDSS) [3]. An exotic form of negative pressure matter called dark energy is used to explain this acceleration. The simplest candidate of dark energy is the cosmological constant Λ, whose energy density remains constant with time $\rho_\Lambda = \Lambda/8\pi G$ and whose equation of motion is also fixed, $w_\Lambda = P_\Lambda/\rho_\Lambda = -1$ (P_Λ is the pressure) during the evolution of the universe. The cosmological model that consists of a mixture of the cosmological constant and cold dark matter is called LCDM model, which provides an excellent explanation for the acceleration of the universe phenomenon and other existing observational data. However, as is well know, this model faces two difficulties, namely, the 'fine-tuning' problem and the 'cosmic coincidence' problem. The former also states: Why the cosmological constant observed today is so much smaller than the Planck scale, while the latter states: Since the energy densities of dark energy and dark matter scale so differently during the expansion of the universe, why they are at the same order today? To alleviate or even solve these two problems, many dynamic dark energy models were proposed such as the quintessence model rely on a scalar field minimally interacting with Einstein gravity. Here 'dynamic' means the equation of state of the dark energy is no longer a constant but slightly evolves with time. Despite considerable works on understanding the dark

energy have been done, the nature of dark energy and its cosmological origin are still enigmatic at present.

On the other hand, the problem of discriminating different dark energy models is now emergent. In order to solve this problem, a sensitive and robust diagnostic for dark energy is a must. The statefinder parameter pair $\{r, s\}$ introduced by Sahni et al. [4] and Alam et al. [5] is proven to be useful tools for this purpose. The statefinder probes the expansion dynamics of the universe through high derivatives of the scale factor $\ddot{a}$ and $\dddot{a}$ and is a natural next step beyond the Hubble parameter $H \equiv \dot{a}/a$ and the deceleration parameter q which depends upon $\ddot{a}$. The statefinder pair $\{r, s\}$ is defined as

$$r \equiv \frac{\dddot{a}}{aH^3}, \qquad s \equiv \frac{r-1}{3(q-1/2)}. \qquad (1)$$

The statefinder pair is a 'geometrical' diagnostic in the sense that it is constructed from a space–time metric directly, and it is more universal than 'physical' variables which depends upon properties of physical fields describing dark energy, because physical variables are, of course, model-dependent. Usually one can plot the trajectories in the r–s plane corresponding to different dark energy models to see the qualitatively different behaviors of them. The spatially flat LCDM scenario corresponds to a fixed point $\{r, s\} = \{1, 0\}$ in this diagram. Departure of a given dark energy model from this fixed point provides a good way of establishing the "distance" of this model from LCDM. As demonstrated in Refs. [4–6] the statefinder can successfully differentiate between a wide variety of dark energy models including the cosmological constant, quintessence, the Chaplygin gas, braneworld models and interacting dark energy models.

One can plot the current locations of the parameters r and s corresponding to different models in statefinder parameter diagrams by theoretical calculating in these models. And on the other

* Address for correspondence: Institute of Theoretical Physics, CAS, Beijing 100080, PR China.
 E-mail address: fengcj@itp.ac.cn.

hand it can also be extracted from experiment data such as the SNAP (SuperNovae Acceleration Probe) data, with which combined the statefinder parameters can serve as a versatile and powerful diagnostic of dark energy in the future. In this Letter, we apply the statefinder diagnostic to the Ricci dark energy model (RDE). It is found that the evolution behavior of the statefinder parameters in this model is much like that in quiessence models, but in a very special case the statefinder diagnostic fails. In Section 2, we will briefly review RDE model, and apply the diagnostic to it in Section 3. In the last section we will give some conclusions. In the case of that the statefinder diagnostic fails, we apply a new diagnostic called the Om diagnostic proposed recently to RDE model in Appendix A.

2. Briefly review on RDE

Holographic principle [7] regards black holes as the maximally entropic objects of a given region and postulates that the maximum entropy inside this region behaves non-extensively, growing only as its surface area. Hence the number of independent degrees of freedom is bounded by the surface area in Planck units, so an effective field theory with UV cutoff Λ in a box of size L is not self consistent, if it does not satisfy the Bekenstein entropy bound [8] $(L\Lambda)^3 \leqslant S_{BH} = \pi L^2 M_{pl}^2$, where $M_{pl}^{-2} \equiv G$ is the Planck mass and S_{BH} is the entropy of a black hole of radius L which acts as an IR cutoff. Cohen et al. [9] suggested that the total energy in a region of size L should not exceed the mass of a black hole of the same size, namely $L^3 \Lambda^4 \leqslant L M_p^2$. Therefore the maximum entropy is $S_{BH}^{3/4}$. Under this assumption, Li [10] proposed the holographic dark energy as follows

$$\rho_\Lambda = 3c^2 M_p^2 L^{-2}, \tag{2}$$

where c^2 is a dimensionless constant. Since the holographic dark energy with Hubble horizon as its IR cutoff does not give an accelerating universe [11], Li suggested to use the future event horizon instead of Hubble horizon and particle horizon, then this model gives an accelerating universe and is consistent with current observation [10,12]. For the recent works on holographic dark energy, see Refs. [13–15].

Recently, Gao et al. [16] have proposed a holographic dark energy model in which the future event horizon is replaced by the inverse of the Ricci scalar curvature, and they call this model the Ricci dark energy model (RDE). This model does not only avoid the causality problem and is phenomenologically viable, but also solve the coincidence problem of dark energy. The Ricci curvature of FRW universe is given by

$$R = -6\left(\dot{H} + 2H^2 + \frac{k}{a^2}\right), \tag{3}$$

where dot denotes a derivative with respect to time t and k is the spatial curvature. They introduced a holographic dark energy proportional to the Ricci scalar

$$\rho_X = \frac{3\alpha}{8\pi G}\left(\dot{H} + 2H^2 + \frac{k}{a^2}\right) \propto R, \tag{4}$$

where the dimensionless coefficient α will be determined by observations and they call this model the Ricci dark energy model. Solving the Friedmann equation they find the result

$$\frac{8\pi G}{3H_0^2}\rho_X = \frac{\alpha}{2-\alpha}\Omega_{m0}e^{-3x} + f_0 e^{-(4-\frac{2}{\alpha})x}, \tag{5}$$

where $\Omega_{m0} \equiv 8\pi G\rho_{m0}/3H_0^2$, $x = \ln a$ and f_0 is an integration constant. Substituting the expression of ρ_X into the conservation equation of energy,

$$p_X = -\rho_X - \frac{1}{3}\frac{d\rho_X}{dx} \tag{6}$$

we get the pressure of dark energy

$$p_X = -\frac{3H_0^2}{8\pi G}\left(\frac{2}{3\alpha} - \frac{1}{3}\right)f_0 e^{-(4-\frac{2}{\alpha})x}. \tag{7}$$

Taking the observation values of parameters they find the $\alpha \simeq 0.46$ and $f_0 \simeq 0.65$ [16]. The evolution of the equation of state $w_X \equiv p_X/\rho_X$ of dark energy is the following. At high redshifts the value of w_X is closed to zero, namely the dark energy behaves like the cold dark matter, and nowadays w_X approaches -1 as required and in the future the dark energy will be phantom. The energy density of RDE during big bang nucleosynthesis (BBN) is so much smaller than that of other components of the universe ($\Omega_X|_{1\,\text{MeV}} < 10^{-6} \ll 0.1$ when $\alpha < 1$), so it does not affect BBN procedure. Further more this model can avoid the age problem and the causality problem. In next section we will study RDE model from the statefinder diagnostic viewpoint.

3. Statefinder diagnostic for RDE

The statefinder parameters can be expressed in terms of the total energy density ρ and the total pressure p in the universe as follows:

$$r = 1 + \frac{9(\rho + p)}{2\rho}\frac{\dot{p}}{\dot{\rho}}, \qquad s = \frac{(\rho + p)}{p}\frac{\dot{p}}{\dot{\rho}}. \tag{8}$$

The deceleration parameter $q \equiv -\ddot{a}/(aH^2)$ can be also expressed in terms of ρ and p

$$q = \frac{1}{2}\left(1 + \frac{3p}{\rho}\right). \tag{9}$$

Assuming the universe is well described by a two component fluid consisting of non-relativistic matter (CDM + baryons) with negligible pressure, i.e. $p_m \ll \rho_m$ and dark energy, namely, $\rho = \rho_m + \rho_X$, and $p \approx p_X$, we obtain the statefinder parameters for RDE model as follows,

$$r = 1 - \left(\frac{1}{\alpha^2}\right)\frac{(2-\alpha)(2\alpha-1)f_0 e^{-(4-\frac{2}{\alpha})x}}{\frac{2}{2-\alpha}\Omega_{m0}e^{-3x} + f_0 e^{-(4-\frac{2}{\alpha})x}},$$

$$s = \frac{2}{3}\left(2 - \frac{1}{\alpha}\right), \tag{10}$$

and the deceleration parameter

$$q = \frac{1}{2}\left(1 - \left(\frac{1}{\alpha}\right)\frac{(2-\alpha)f_0 e^{-(4-\frac{2}{\alpha})x}}{\frac{2}{2-\alpha}\Omega_{m0}e^{-3x} + f_0 e^{-(4-\frac{2}{\alpha})x}}\right). \tag{11}$$

From Eq. (10), one can see that $s = 0$, $r = 1$ if $\alpha = 0.5$ and no matter what value f_0 is, and this point in the r–s plane is the very fixed point corresponding to LCDM model. Thus, the statefinder diagnostic fails to discriminate between the LCDM and RDE model in this case. If $\alpha < 0.5$, then the trajectory will lying in the region $r > 1$, $s < 0$.

As an example, we plot the statefinder diagrams in the r–s plane and r–q plane as a complementarity with $\alpha = 0.46$ and $f_0 = 0.65$ obtained in Ref. [16] in Figs. 1 and 2.

In Fig. 1, LCDM scenario corresponds to a fixed point $s = 0$, $r = 1$, and the SCDM (standard cold matter) scenario corresponds to the point $s = 1$, $r = 1$. For RDE model, the trajectory is a vertical segment, i.e. s is a constant during the evolution of the universe, while r monotonically increases from 1 to $1 - (2-\alpha)(2\alpha-1)/\alpha^2 \approx 1.58$. The location of today's point is $s = -0.12$, $r = 1.38$, thus the 'distance' from RDE model to LCDM model can be easily identified in this diagram. The trajectories for the so-called 'quintessence' model (w is a constant) are also vertical segments, but in that model, r decreases monotonically from 1 to $1 + 9w(1+w)/2$ while s remains constant at $1 + w$ [4,5].

Trajectory in the r−s plane
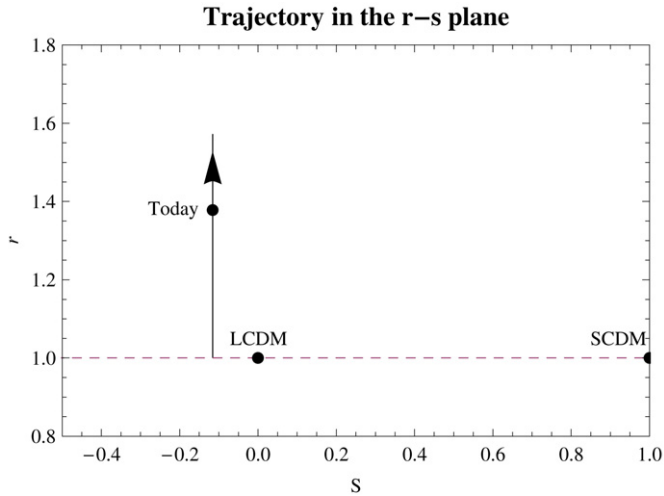
Fig. 1. Evolution trajectory in the statefinder r–s plane for RDE with $\alpha = 0.46$ and $f_0 = 0.65$.

Trajectory in the r−q plane
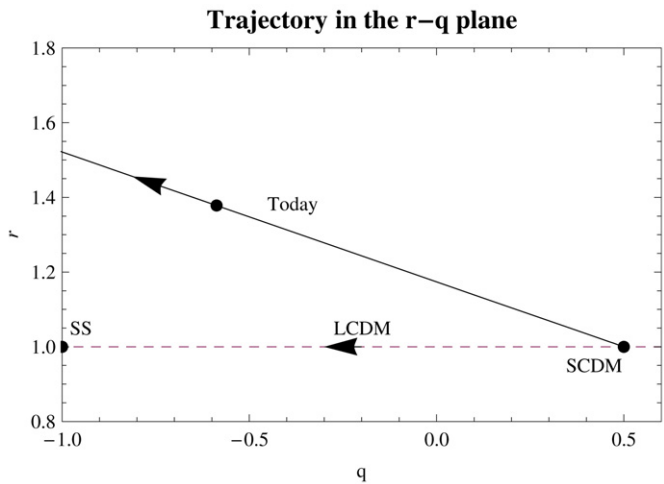
Fig. 2. Evolution trajectory in the statefinder r–q plane for RDE with $\alpha = 0.46$ and $f_0 = 0.65$. The solid line represents the RDE model, and the dashed line the LCDM as comparison. The location of today's point is $(-0.59, 1.38)$.

In fact, the statefinder diagnostic can also discriminate between other dark energy models effectively. For example, the trajectories for the Chaplygin gas and the quintessence (inverse power low) models are similar to arcs of a parabola (downward and upward) lying in the regions $s < 0$, $r > 1$ and $s > 0$, $r < 1$ respectively. For holographic dark energy model with the future event horizon as IR cutoff, commences its evolution from the point $s = 2/3$, $r = 1$, through an arc segment, and ends it at LCDM fixed point in the future [6]. Therefore, the distinctive trajectories corresponding to various dark energy scenario in the r–s plane demonstrate quite strikingly the contrasting behaviors of dark energy models.

In Fig. 2, we clearly see that both LCDM scenario and RDE model commence evolving from the same point in the past $q = 0.5$, $r = 1$, which corresponds to a matter dominated SCDM universe. However, in LCDM model the trajectory will end their evolution at the point $q = -1$, $r = 1$ which corresponds to a steady state cosmology (SS), i.e. the de Sitter expansion, while that in RDE model does not. In Ref. [6], the trajectory in holographic dark energy model with the future event horizon (HDE) has the same starting point and the same ending point as that in LCDM model. Thus, RDE model is also different from HDE model from the statefinder viewpoint.

If $\alpha > 0.5$, the sign of s becomes positive and $r < 1$ if α is also smaller than 2, but the value of r will lager than 1 if $\alpha > 2$, see Eq. (10). Thus, the determining of the value of α is a key point to the feature of RDE model and we hope the future high precision experiments may provide sufficiently large amount of precise data to be capable of determining the value of α.

4. Conclusions

In this Letter, we have apply the statefinder diagnostic to the Ricci dark energy model, and plot the trajectories in the r–s and r–q planes in the case of $\alpha = 0.46$ and $f_0 = 0.65$. Here we have used the values of α and f_0 that founded in Ref. [16], but other values are also possible. Different values of α will determine different evolutions of the statefinder parameters, so the determining of α from more precise data provided by future experiments will be needed. In a very special case that $\alpha = 0.5$, the statefinder pair $\{r, s\}$ fails to discriminate LCDM model and RDE model, because they give the same fixed point $r = 1$, $s = 0$ in the r–s diagram. The difference of these two models is the evolution of the equation of state w, which is a constant that equals -1 in the former and a time-dependent variable in the latter. Recently, a new diagnostics called the *Om* diagnostic of dark energy is proposed in Ref. [17]. In Appendix A, we will apply this diagnostic to RDE model in the case of $\alpha = 0.5$ in order to differentiate LCDM model and RDE model. The result indicates that this new diagnostic really works well for this purpose.

Although we have showed these two diagnostics of DE can differ RDE and LCDM in an ideal case, the observational uncertainties should be considered also. According to the estimations of parameters $\langle r \rangle$ and $\langle s \rangle$, which defined as

$$\langle r \rangle = \frac{1}{1000} \sum_{i=1}^{1000} r_i, \qquad \langle s \rangle = \frac{1}{1000} \sum_{i=1}^{1000} s_i, \tag{12}$$

where 1000 stands for numbers of data sets from SNAP [4,5], we can ruled out a number of tracker and quiessence model with constant equation of state $w \geqslant -0.9$ at the 3σ level if the value of Ω_{m0} is known exactly. However, according to the current observations it is not good enough to determine Ω_{m0} as discussed in Ref. [17]. Thus, for the statefinder diagnostic, it is very important to determine the value of Ω_{m0} and the values of parameters of the model by the future observations and in our case it is the value of α in RDE.

The new diagnostic *Om* can be determined independent of the value of Ω_{m0}, then it is better than the statefinder diagnostic. However, it could only distinguish between DE models at 1σ level [17], and it is consistent with LCDM model without excluding dynamic DE models like phantom, quintessence, RDE, etc., by using the current data. Thus, further high precision data are highly needed.

Acknowledgements

Appendix A

The definition of the *Om* diagnostic is [17]

$$Om(x) \equiv \frac{h^2(x) - 1}{e^{-3x} - 1}, \tag{A.1}$$
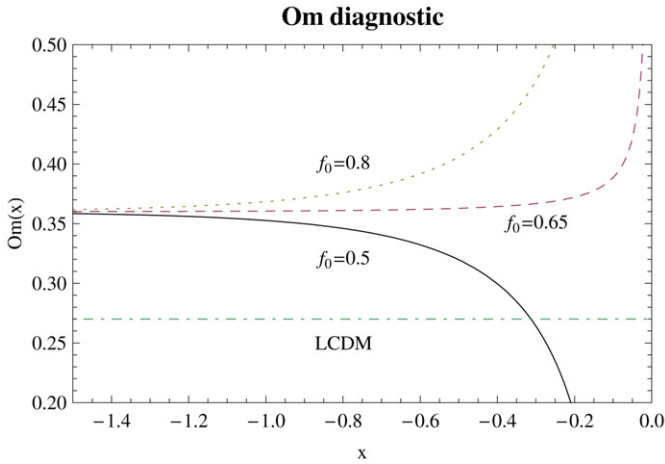
Om diagnostic

Fig. 3. The *Om* diagnostic for RDE with $\alpha = 0.5$, $\Omega_{m0} = 0.27$ as well as $f_0 = 0.5$, 0.65 and 0.8, respectively.

where $h(x) \equiv H(x)/H_0$. For dark energy with a constant dark energy equation of state $w = \text{const}$ in the spatially flat universe,

$$h^2(x) = \Omega_{m0}e^{-3x} + (1 - \Omega_{m0})e^{-3(1+w)x}. \tag{A.2}$$

Consequently,

$$Om(x) = \Omega_{m0} + (1 - \Omega_{m0})\frac{e^{-3(1+w)x} - 1}{e^{-3x} - 1}, \tag{A.3}$$

from where we get

$$Om(x) = \Omega_{m0} \tag{A.4}$$

in the LCDM model. Authors in Ref. [17] conclude that: $Om(x) - \Omega_{m0} = 0$, if and only if dark energy is a cosmological constant.

From Eq. (8) in [16], we get

$$h^2(x) = \frac{2}{2-\alpha}\Omega_{m0}e^{-3x} + f_0 e^{-(4-\frac{2}{\alpha})x} \tag{A.5}$$

in RDE model, then the *Om* diagnostic for it is

$$Om(x) = \frac{\frac{2}{2-\alpha}\Omega_{m0}e^{-3x} + f_0 e^{-(4-\frac{2}{\alpha})x} - 1}{e^{-3x} - 1}. \tag{A.6}$$

As an example, we take $\alpha = 0.5$ and $\Omega_{m0} = 0.27$ to plot the evolutions of $Om(x)$ corresponding to $f_0 = 0.5$, 0.65 and 0.8 in Fig. 3.

Thus, one can easily find the difference between the LCDM model and RDE model from Fig. 3. Especially the difference is much larger near present, i.e. $x \sim 0$. Here f_0 plays a important role to determine the evolution of *Om*, so f_0 value is also hoped to be determined from future precise data as α.

References

[1] A.G. Riess, et al., Supernova Search Team Collaboration, Astron. J. 116 (1998) 1009, astro-ph/9805201;
    S. Perlmutter, et al., Supernova Cosmology Project Collaboration, Astrophys. J. 517 (1999) 565, astro-ph/9812133.
[2] D.N. Spergel, et al., WMAP Collaboration, Astrophys. J. Suppl. 170 (2007) 377, astro-ph/0603449;
    E. Komatsu, et al., WMAP Collaboration, arXiv: 0803.0547 [astro-ph].
[3] J.K. Adelman-McCarthy, et al., SDSS Collaboration, arXiv: 0707.3413 [astro-ph].
[4] V. Sahni, T.D. Saini, A.A. Starobinsky, U. Alam, JETP Lett. 77 (2003) 201, Pis'ma Zh. Eksp. Teor. Fiz. 77 (2003) 249, astro-ph/0201498.
[5] U. Alam, V. Sahni, T.D. Saini, A.A. Starobinsky, Mon. Not. R. Astron. Soc. 344 (2003) 1057, astro-ph/0303009.
[6] W. Zimdahl, D. Pavon, Gen. Relativ. Gravit. 36 (2004) 1483, gr-qc/0311067;
    X. Zhang, Phys. Lett. B 611 (2005) 1, astro-ph/0503075;
    X. Zhang, Int. J. Mod. Phys. D 14 (2005) 1597, astro-ph/0504586;
    M.P. Dabrowski, Phys. Lett. B 625 (2005) 184, gr-qc/0505069;

P.x. Wu, H.w. Yu, Int. J. Mod. Phys. D 14 (2005) 1873, gr-qc/0509036;
    M.G. Hu, X.H. Meng, Phys. Lett. B 635 (2006) 186, astro-ph/0511615;
    E.E.O. Ishida, Braz. J. Phys. 35 (2005) 1172, astro-ph/0609614;
    M.R. Setare, J. Zhang, X. Zhang, JCAP 0703 (2007) 007, gr-qc/0611084;
    B.R. Chang, H.Y. Liu, L.X. Xu, C.W. Zhang, Y.L. Ping, JCAP 0701 (2007) 016, astro-ph/0612616;
    Y. Shao, Y. Gui, Mod. Phys. Lett. A 23 (2008) 65, gr-qc/0703111;
    Z.L. Yi, T.J. Zhang, Phys. Rev. D 75 (2007) 083515, astro-ph/0703630;
    B. Chang, H. Liu, L. Xu, C. Zhang, Mod. Phys. Lett. A 23 (2008) 269, arXiv: 0704.3670 [astro-ph];
    B. Chang, H. Liu, L. Xu, C. Zhang, arXiv: 0704.3768 [astro-ph];
    J. Zhang, X. Zhang, H. Liu, Phys. Lett. B 659 (2008) 26, arXiv: 0705.4145 [astro-ph];
    H. Wei, R.G. Cai, Phys. Lett. B 655 (2007) 1, arXiv: 0707.4526 [gr-qc];
    W. Zhao, arXiv: 0711.2319 [gr-qc];
    D.J. Liu, W.Z. Liu, Phys. Rev. D 77 (2008) 027301, arXiv: 0711.4854 [astro-ph];
    G. Panotopoulos, Nucl. Phys. B 796 (2008) 66, arXiv: 0712.1177 [astro-ph];
    Z.G. Huang, X.M. Song, H.Q. Lu, W. Fang, Astrophys. Space Sci. 315 (2008) 175, arXiv: 0802.2320 [hep-th];
    Z.G. Huang, H.Q. Lu, arXiv: 0802.2321 [hep-th];
    W.Z. Liu, D.J. Liu, arXiv: 0803.4039 [astro-ph].
[7] R. Bousso, Rev. Mod. Phys. 74 (2002) 825, hep-th/0203101.
[8] J.D. Bekenstein, Phys. Rev. D 7 (1973) 2333;
    J.D. Bekenstein, Phys. Rev. D 23 (1981) 287.
[9] A.G. Cohen, D.B. Kaplan, A.E. Nelson, Phys. Rev. Lett. 82 (1999) 4971, hep-th/9803132.
[10] M. Li, Phys. Lett. B 603 (2004) 1, hep-th/0403127.
[11] S.D.H. Hsu, Phys. Lett. B 594 (2004) 13, hep-th/0403052.
[12] Q.G. Huang, M. Li, JCAP 0408 (2004) 013, astro-ph/0404229;
    Q.G. Huang, M. Li, JCAP 0503 (2005) 001, hep-th/0410095.
[13] X. Zhang, F.Q. Wu, Phys. Rev. D 76 (2007) 023502, astro-ph/0701405;
    Y.S. Myung, Phys. Lett. B 649 (2007) 247, gr-qc/0702032;
    H.b. Zhang, W. Zhong, Z.H. Zhu, S. He, Phys. Rev. D 76 (2007) 123508, arXiv: 0705.4409 [astro-ph];
    Z.Y. Sun, Y.G. Shen, Int. J. Theor. Phys. 46 (2007) 877;
    Y.S. Myung, Phys. Lett. B 652 (2007) 223, arXiv: 0706.3757 [gr-qc];
    C. Feng, B. Wang, Y. Gong, R.K. Su, JCAP 0709 (2007) 005, arXiv: 0706.4033 [astro-ph];
    H. Wei, S.N. Zhang, Phys. Rev. D 76 (2007) 063003, arXiv: 0707.2129 [astro-ph];
    B. Guberina, arXiv: 0707.3778 [gr-qc];
    B.C. Paul, P. Thakur, A. Saha, arXiv: 0707.4625 [gr-qc];
    J.f. Zhang, X. Zhang, H.y. Liu, Eur. Phys. J. C 52 (2007) 693, arXiv: 0708.3121 [hep-th];
    C.J. Feng, arXiv: 0709.2456 [hep-th];
    Y.Z. Ma, Y. Gong, arXiv: 0711.1641 [astro-ph];
    R. Horvat, arXiv: 0711.4013 [gr-qc];
    E. Elizalde, S. Nojiri, S.D. Odintsov, P. Wang, Phys. Rev. D 71 (2005) 103504, hep-th/0502082;
    S. Nojiri, S.D. Odintsov, Gen. Relativ. Gravit. 38 (2006) 1285, hep-th/0506212.
[14] H.M. Sadjadi, JCAP 0702 (2007) 026, gr-qc/0701074;
    M.R. Setare, JCAP 0701 (2007) 023, hep-th/0701242;
    M.R. Setare, E.C. Vagenas, arXiv: 0704.2070 [hep-th];
    J. Zhang, X. Zhang, H. Liu, Phys. Lett. B 659 (2008) 26, arXiv: 0705.4145 [astro-ph];
    Q. Wu, Y. Gong, A. Wang, J.S. Alcaniz, Phys. Lett. B 659 (2008) 34, arXiv: 0705.1006 [astro-ph];
    K.Y. Kim, H.W. Lee, Y.S. Myung, Mod. Phys. Lett. A 22 (2007) 2631, arXiv: 0706.2444 [gr-qc];
    M.R. Setare, arXiv: 0708.3284 [hep-th].
[15] E.N. Saridakis, Phys. Lett. B 660 (2008) 138, arXiv: 0712.2228 [hep-th];
    E.N. Saridakis, JCAP 0804 (2008) 020, arXiv: 0712.2672 [astro-ph];
    X. Wu, Z.H. Zhu, Phys. Lett. B 660 (2008) 293, arXiv: 0712.3603 [astro-ph];
    E.N. Saridakis, Phys. Lett. B 661 (2008) 335, arXiv: 0712.3806 [gr-qc];
    A.A. Sen, D. Pavon, arXiv: 0801.0280 [astro-ph];
    M. Li, C. Lin, Y. Wang, arXiv: 0801.1407 [astro-ph];
    K. Karwan, JCAP 0805 (2008) 011, arXiv: 0801.1755 [astro-ph];
    M.R. Setare, E.C. Vagenas, arXiv: 0801.4478 [hep-th];
    A.J.M. Medved, arXiv: 0802.1753 [hep-th];
    Y.S. Myung, M.G. Seo, arXiv: 0803.2913 [gr-qc];
    B. Nayak, L.P. Singh, arXiv: 0803.2930 [gr-qc];
    L. Xu, J. Lu, arXiv: 0804.2925 [astro-ph];
    K.Y. Kim, H.W. Lee, Y.S. Myung, arXiv: 0805.3941 [gr-qc];
    C.J. Feng, arXiv: 0806.0673 [hep-th];
    H. Mohseni Sadjadi, N. Vadood, arXiv: 0806.2767 [gr-qc];
    R. Horvat, arXiv: 0806.4825 [gr-qc];
    N. Cruz, S. Lepe, F. Pena, J. Saavedra, arXiv: 0807.3854 [gr-qc];
    Y. Bisabr, arXiv: 0808.1424 [gr-qc].
[16] C. Gao, X. Chen, Y.G. Shen, arXiv: 0712.1394 [astro-ph].
[17] V. Sahni, A. Shafieloo, A.A. Starobinsky, arXiv: 0807.3548 [astro-ph].